Performance Evaluation of Sun Tracking Control Systems using IMC and PID Controllers

Ifetola Damilola Madaki[1], Taliha Abiodun Folorunso[2], Jibril Abdullahi Bala[2], Adeyinka Peace Adedigba[2], Eustace M. Dogo[1]

[1]*Department of Computer Engineering,*
[2]*Department of Mechatronics Engineering,*
School of Electrical Engineering and Technology,
Federal University of Technology, Minna.
Email: ifetola.pg2115780@st.futminna.edu.ng

ABSTRACT

The inadequate supply of electricity for illumination has made many industries, organizations, and households resort to alternative energy sources, one of which includes solar energy. In comparison to other renewable sources of energy, the idea of employing photovoltaic panels for solar energy conversion into electrical energy remains a widespread choice. However, the amount of power a solar panel can produce is reduced due to the sun's constant shift in angle with respect to the earth. In this work, we evaluate the performance response of the STS using the transient response, Integral Absolute Error (IAE) and Integral Square Error (ISE) of the IMC and PID controller using MATLAB. The results obtained shows that, the PID outperforms the IMC in terms of IAE, ISE and Rise time, while the IMC outperforms the PID in terms of Settling time and system overshoot.

Keywords: *Integral Absolute Error (IAE), Integral Square Error (ISE), Internal Model Controller (IMC), Proportional-Integral-Derivative (PID), Sun Tracking System (STS).*

1   INTRODUCTION

Globally, there is a general push away from fossil-based energy sources towards renewable energy technologies and sources. This is in effort to combat the depleting ozone layer and its attendant climate issues. Over the years, renewable energy sources and their associated technologies have shown a positive impact in changing the narratives with regard to reducing the effects of energy generation on climate change (Auken, Guijarro, & Vries, 2022; Marwan & Anshar, 2020; Racharla & Rajan, 2017).

In comparison to other renewable energy sources, solar energy remains one among the easily tapped energy sources for power generation, due the to ease of harvesting using photovoltaic (PV) cells (Auken et al., 2022). However, the amount of energy generated depends on the exposure of the PV Cells to solar radiation. Hence, for optimal performance, there must be maximum exposure of the PV cells to solar radiation (Racharla & Rajan, 2017).

In the quest to guarantee the maximum exposure of PV Cells to maximum solar radiation, a number of approaches have been implemented in literature with the solar tracking system being the most prominent (Hanwate & Hote, 2018). Albeit the efficacy of this approach is dependent on its ability to continuously track the maximum solar radiation through the tilt angle of the PV cells in line with solar movement. The solar tracking system (STS) is an electromechanical device that positions the PV Cells at an angle relative to the sun for optimal solar radiation (Hanwate & Hote, 2018). The tracking system also allows the movement of the PV Cells through the angle of tilt/inclination in line with the solar system's movement. To maximize the power extraction of the solar system, there exist three major approaches of controlling the tilt angle of the tracking system. These approaches include, the active, passive and hybrid approaches (Arif, Hossen, Ramana Murthy, & Armanur Rahaman, 2018). The efficacy of all three approaches lies in the ability of their controllers to regulate the tilt angle accordingly with the solar system.

The Proportional-Integral-Derivative (PID) controller exist as one of the simplest and easiest form of controllers to implement yet widely used for varying control applications (Arif et al., 2018; Hanwate & Hote, 2018; Oladayo & Titus, 2016; Rawat, Jha, &

Kumar, 2020). The essential features of the PID Controller lie in the ease and simplicity of tuning (Folorunso, Bala, Adedigba, & Aibinu, 2021). The PID controller has also been applied in the control of single, dual, and multiple-axis tracking solar systems for optimal performance (Folorunso et al., 2021; Rawat et al., 2020; Suboh, Er, & Sardi, 2022). Another variant of PID controller based on the tuning techniques has also been applied to track solar radiation (Arif et al., 2018; Hanwate & Hote, 2018; Rawat et al., 2020). The Internal Model Controller (IMC) is another type of controller that has been used in the control of solar tracking systems (Suboh et al., 2022). The IMC has some inherent characteristics that ensure its robustness and good tracking performance for several control applications (Folorunso et al., 2021; Zeng et al., 2020). Furthermore, the performance of the STS is solely dependent on the ability of the controller adapted to control its movement accordingly. However, the performance of the controller is also primarily dependent on the selection of appropriate controller gains. In this paper, the performance evaluation of the PID and IMC controllers in controlling the STS is investigated. This is with the view of obtaining the most optimal in tracking the conventional STS.

The rest of this paper are organized into four sections. Section 2, briefly describes the STS, the system model, and the design. Section 3, presents results and discussion. Lastly, Section 4, conclusion and recommendations for future works are presented.

2 METHODOLOGY

The structure of a typical STS is as depicted in Figure 1, wherein the principal inputs for tracking are the temperature and irradiance as presented (Arif et al., 2018). The goal of the tracking system is to ensure that the exposure to the input (temperature and irradiance) is always maximum.
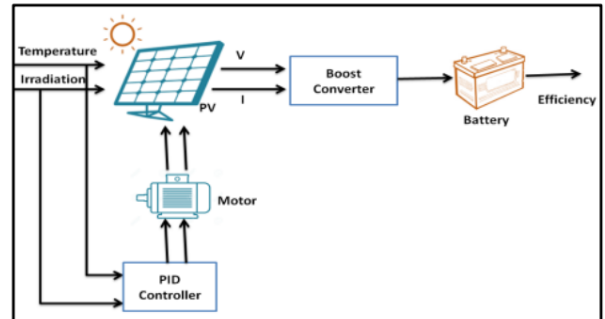

Figure 1: Representation of the STS (Rawat et al., 2020)

In Figure 2, the block diagram representing the STS is presented. The electric motors are the primary mover in the sun tracking system, the rotation of the solar cells is achieved by controlling the motor. A light-sensitive device, such as a Light Dependent Resistor (LDR), is utilized as the input sensor unit in a solar tracking system which produces the voltage required to power the motor; the output provides the angular displacement of the electric motor, which represents the motion of the STS.
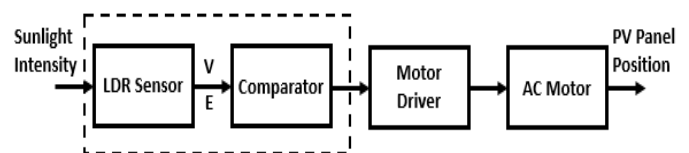

Figure 2: Simplified block diagram of a solar tracker (Wang & Lu, 2013)

2.1 SYSTEM MODELLING

In this section, the mathematical model of the STS is presented as a function of the DC motor. The STS IS modelled using the typical DC motor (Electromechanical System) as depicted in Figure 3. The Solar Tracker system can be identified based on the behavior of input applied to it. The mathematical model is derived from the real performance of the system input.
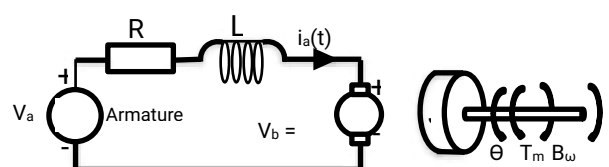
Figure 3: Model diagram of the electromechanical system (Olaniyi, Folorunso, Kolo, Arulogun, & Bala, 2015)

Where:
T_m = Torque of motor
v_a = Applied voltage
J = inertia of the rotor
ω = Angular Velocity
vb = Back EMF
B = co-efficient of viscous friction
K_t = Torque Constant
K_b = Back EMF constant
θ = Angular displacement
$i_a(t)$ = Armature current
R = Resistance of the armature
L = Inductance of the armature
Td = Disturbance Torque

In a magnetic field, the voltage of the rotating, current-carrying armature, is proportional to the speed. Therefore,

$$V_b(t) = K_b \frac{d\theta_m}{dt} \qquad \text{i}$$

Taking the Laplace transform, we get

$$V_b(s) = k_{bS_{\theta m(s)}} \qquad \text{ii}$$

The Laplace-transform equation of the loop around the armature circuit gives the relationship between the applied armature voltage, the armature current, $i_a(t)$, $e_a(t)$, and the back emf, $V_b(t)$.

$$R_a i_a(s) + L_a s i_a(s) + V_b(s) = E_s(s) \qquad \text{iii}$$

The torque of the motor output is proportional to the current of the armature. Thus,

$$T_m(s) = K_t I_a(s) T_m \qquad \text{iv}$$

Rearranging Equation (iv) gives,

$$i_a(s) = \frac{1}{T_m}(s) \qquad \text{v}$$

Substituting Equations (ii) and (iv) into (iii), gives;

$$\frac{(R_a L_a s)\, T_m(s)}{k_t} + K_b s \theta_m(s)$$
vi

Dm, which comprises the armature and load viscous damping, is the equivalent viscous damping at the armature.

$$T_m(s) = \left(J_m s^2 + D_m s\right)\theta_m(s) \qquad \text{vii}$$

Substituting Eq. (vii) into Equation (vi) yields
$$\frac{(R_a + L_a s)\left(J_m s^2 + D_m s\right)\theta_m(s)}{K_t} + K_b s \theta_m(s) = E_a(s) \qquad \text{e}$$
viii   Error

Simplifying, the transfer function, $\theta m(s)/Ea(s)$, gives;

$$\frac{\theta_m(s)}{E_a(s)} = \frac{\frac{K}{R_a J_m}}{s\left[s + \frac{1}{J_m}\left(D_m + \frac{K_t k_b}{R_a}\right)\right]}$$
ix

Table 1 shows the parameters of the DC servo motor utilized in this study. The motor under consideration is the M600 series DC servo motor by Mclennan.

Table 1: Values used based on the proposed DC motor for the sun tracking system (*M600 Series Dimensions : Mm M600 Series*, 2019.).

Parameters	Values
K_t	0.0816NM/Amp
K_b	0.0816NM/Amp
D_m	0.0000816MN/rad sec
J_m	0.012Kg/m2
R_a	0.6Ω

Substituting these values into equation ix, we have:

$$\frac{\theta_m(s)}{E_a(s)} = \frac{11.3}{s^2 + 0.992s}$$
x

2.2 PID Control System Design

The Proportional-Integral-Derivative (PID) controller is a closed-looped and is statistically among the most widely used controllers in the engineering sector. The PID controller comprises of three components which are the Proportional term (Kp), the Integral term (Ki) and the Derivative term (Kd). The function of each term is as stated below:

- Proportional Gain (Kp): The system speed is increased since the output is proportional to the error value.

- Integral Gain (Ki): Steady-state error is reduced by using an integrator to compensate for low frequency

- Derivative Gain (Kd): Enhances transient response through high-frequency differentiator compensation.

To make sure that the output of the control system track movement of the sun efficiently, the PID parameters must be tuned. This requires modifying the proportional, integral, and derivative gains. Figure 4 represents a PID controller.

Figure 4: Diagram of the PID controller (Bala, 2022)

$$U(t) = K_p e(t) + K_i \int e(t)\, d(t) + k_p \frac{d_e}{d_t}$$

xi

$$G_{PID}(s) = K_p + \frac{K_i}{s} + K_d(s)$$ xii

Where;

U_t = PID Control Variable

K_p = Proportional gain

e_t = Error value

K_i = Integral gain

d_e = Change in the error value

Parameter	Value
Proportional Gain (Kp)	0.1818
Integral Gain (Ki)	0.0419
Derivative Gain (Kd)	0.1375

d_t = Change in time

The PID tuner app in MATLAB was used in tuning the PID controller. The parameters generated using the application are presented in Table 2.

Table 2: PID Tuning Parameters

2.3 INTERNAL MODEL CONTROLLER (IMC)

Garcia and Morari proposed IMC in 1982, and it has since received researchers' interest because of its ease of use, robustness, powerful tracking performance, and simplicity of tuning. The IMC also features an optimal control characteristic of zero(0) steady-state error as well as simplicity of parameter adjustment (Balaa, Olaniyi, Folorunso, & Arulogund, 2020), (Folorunso et al., 2021). Figure 5 shows the block diagram of a typical IMC control process.
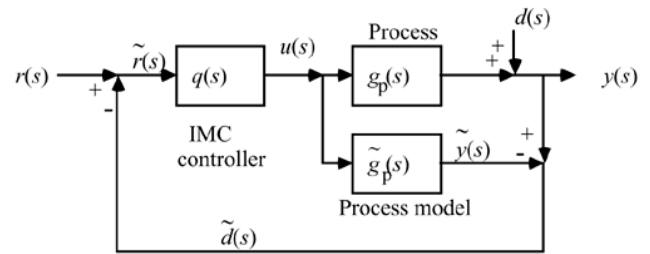

Figure 5: An IMC Control Process (Zeng et al., 2020).

$$G_c(s) = \frac{G_{IMC}(s)}{1 - G_{IMC}(s)G_p(s)}$$ xiii

Where;
G_{IMC} = IMC controller,
Gp = process,
Ĝp = process model and
Gd = external disturbance.

$$G_{IMC}(s) = G^{-1}_p(s)F(s)$$ xiv

Where;
F(s) = Filter and
G^{-1}_p = Inverse of the plant model

$$F(s) = \frac{1}{(1+\lambda s)^n}$$ xv

Where n is adequately enormous to make the controller suitable and λ is the tuning parameter in charge of the speed of response and robustness. λ also deals with close-loop performance and

modelling errors. An n value was selected because the plant model is a second-order system while a λ value of 1 was selected for the IMC system.

3 RESULTS AND DISCUSSION

3.1 PID CONTROLLER

Figure 6 presents the system block diagram in Simulink and Figure 7 presents the system response of the PID controller.
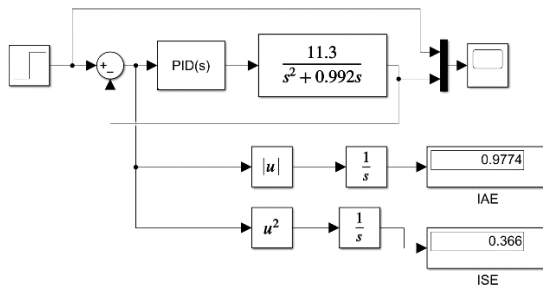

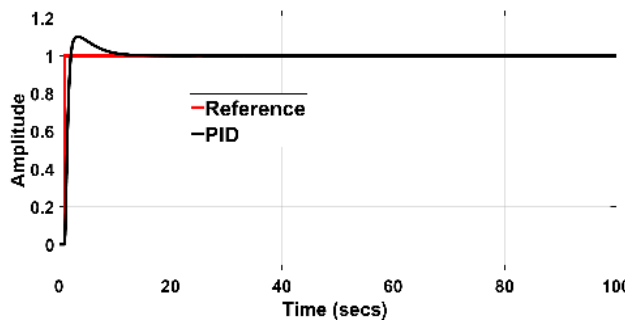Figure 6: PID Simulink block representation of the sun tracking system

Figure 7: PID System Response of the sun tracking system

The graph in Figure 7 was obtained from the oscilloscope which serves as an output to the control system using MATLAB. It shows the system response, transient and steady-state response and the system behavior. From the figure, it was observed that the system has a rise time of

753.072ms. This implies that it takes the system 0.753 seconds to rise from 10% to 90% of the final step value. Additionally, the system exhibited a settling time of 15s. This indicates that the system took 15 seconds to settle within 2% of the final value. Furthermore, the system showed an overshoot of 10.6%, which implies that the system response went over the final step value by 10.6% before eventually settling down to the desired value. The system exhibited an IAE of 0.99774 and an ISE of 0.366, implying the errors the system accumulated over the simulation time of 100 seconds.

3.2 IMC

Figure 8 presents the IMC system block diagram in Simulink and Figure 9 presents the system response of the IMC.
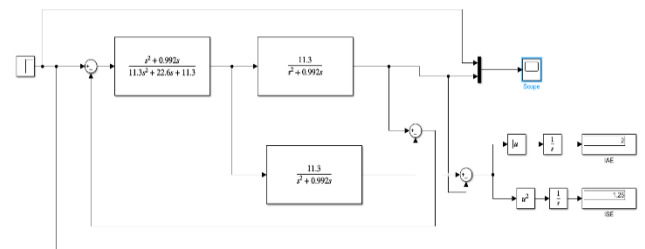

Figure 8: IMC Simulink block representation of the sun tracking system
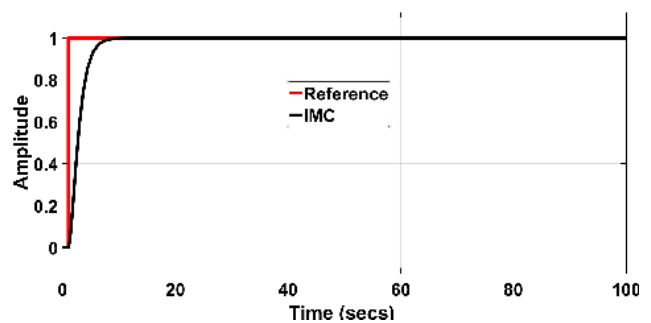

Figure 9: IMC graphical representation of the sun tracking system

The graph in Figure 9 was obtained from the oscilloscope which serves as an output to the control system using MATLAB. It shows the system response, transient and steady-state response and the system behavior. From the figure, it was observed that the system has a rise time of 3.376s. This implies that it takes the system 3.376s seconds to rise from 10% to 90% of the final step value. Also, the system exhibited a settling time of 9s. This shows that the system took 9 seconds to settle within 2% of the final value. Furthermore, the system showed an overshoot of approximately 0%, which implies that the system response went over the final step value by approximately 0% which is almost negligible before settling down to the desired value. The system exhibited an IAE of 2 and an ISE of 1.25, implying the errors the system accumulated over the simulation time of 100 seconds.

3.3 Comparative results

The combined system responses of the IMC and PID controllers in relation to the step input is presented in Figure 10. In addition, Table 3 shows a comparative analysis between the IMC and PID controller.
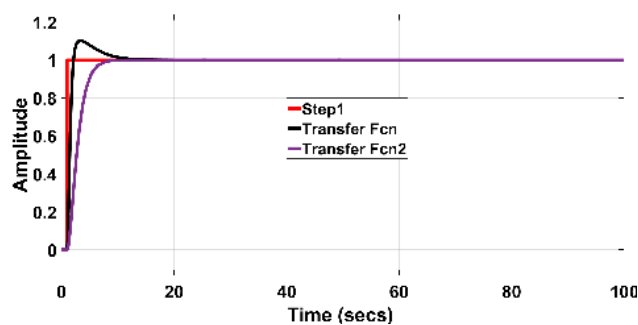

Figure 10: Combined System Response of IMC and PID Controllers

Table 3: Comparative result of the IMC and PID controller

	Rise Time (secs)	Settling time (secs)	Overshoot (%)	Integral Absolute Error (IAE)	Integral Square Error (ISE)
PID	0.753	15	10.6	0.99774	0.366
IMC	3.376	9	0	2	1.25

From Figure 10 and Table 3, it can be seen that the PID control system had a lower rise time than the IMC system. This implies the PID system will reach its desired set point faster than the IMC-based system. In terms of the settling time, however, the IMC had a lower value than the PID implying the IMC settles faster to the final step value. The IMC had a very low overshoot of approximately 0% which is characteristic of the IMC. On the other hand, the PID had an overshoot of 10.6%. In the cases of the ISE and IAE, the PID exhibited lower error values than the IMC. This implies the PID showed more accurate tracking performance over the simulation time.

4   CONCLUSION

In conclusion, the performance evaluation of the IMC and PID Control system for the STS was carried out successfully. The results obtained show that in terms of IAE, ISE and Rise time, the PID outperforms the IMC, while the IMC outperforms the PID in terms of settling time and system overshoot. This implies that the controllers can be successfully implemented in a STS depending on the preferred performance. If the speed of response is preferred with minimal tracking errors, then the PID is recommended. However, if a lower overshoot is preferred, then the IMC provides that performance. Future works will examine the effect of Optimization algorithms on PID and IMC systems for solar tracking.

REFERENCE

Arif, E., Hossen, J., Ramana Murthy, G., & Armanur Rahaman, M. (2018). *A novel PID controller based solar panel tracking system*. (April),

115–116.

Auken, V., Guijarro, M., & Vries, D. (2022). *Consumer response to adoption and demand for energy saving bulbs in nigeria.* 8(1).

Bala, J. A. (2022). *Mce 514 : Modern.* (Bala, J. A. (2022.). MCE 514 : Modern Control Systems, lecture notes, Federal University of Technology Minna, Nigeria.).

Balaa, J. A., Olaniyi, O. M., Folorunso, T. A., & Arulogund, O. T. (2020). *Optimally Tuned IMC and PID Controllers on a.* 6(4).

Folorunso, T. A., Bala, J. A., Adedigba, A. P., & Aibinu, A. M. (2021). Genetic Algorithm Tuned IMC-PI Controller for Coupled Tank Based Systems. *2021 1st International Conference on Multidisciplinary Engineering and Applied Science, ICMEAS 2021,* (Imc), 72–77. https://doi.org/10.1109/ICMEAS52683.2021.9692406

Hanwate, S. D., & Hote, Y. V. (2018). Design of PID controller for sun tracker system using QRAWCP approach. *International Journal of Computational Intelligence Systems,* 11(1), 133–145. https://doi.org/10.2991/ijcis.11.1.11

M600 series Dimensions : mm M600 series. (n.d.). *173*(0).

Marwan, ., & Anshar, M. (2020). *PID Controller Design for Solar Tracking System.* (Conrist 2019), 72–77. https://doi.org/10.5220/0009431400720077

Oladayo, B. O., & Titus, A. O. (2016). Development of Solar Tracking System Using Imc-Pid Controller American Journal of EnginOladayo, B. O., & Titus, A. O. (2016). Development of Solar Tracking System Using Imc-Pid Controller American Journal of Engineering Research (AJER). American Journal. *American Journal of Engineering Research (AJER),* 5(5), 1–8.

Olaniyi, O. M., Folorunso, T. A., Kolo, J. G., Arulogun, O. T., & Bala, J. A. (2015). *Towards The Development of a Mobile Intelligent Poultry Feed Dispensing System Using Particle Swarm Optimized PID Control Technique.* 8(3), 93–106.

Racharla, S., & Rajan, K. (2017). Solar tracking system–a review. *International Journal of Sustainable Engineering,* 10(2), 72–81. https://doi.org/10.1080/19397038.2016.1267816

Rawat, A., Jha, S. K., & Kumar, B. (2020). Position controlling of Sun Tracking System using optimization technique. *Energy Reports,* 6, 304–309. https://doi.org/10.1016/j.egyr.2019.11.079

Suboh, S. M., Er, L. C., & Sardi, J. (2022). Power Controller for Dual-axis Solar Tracking System using PID. *Journal of Physics: Conference Series,* 2312(1). https://doi.org/10.1088/1742-6596/2312/1/012068

Wang, J. M., & Lu, C. L. (2013). Design and implementation of a sun tracker with a dual-axis single motor for an optical sensor-based photovoltaic system. *Sensors (Switzerland),* 13(3), 3157–3168. https://doi.org/10.3390/s130303157

Zeng, W., Zhu, W., Hui, T., Chen, L., Xie, J., & Yu, T. (2020). An IMC-PID controller with Particle Swarm Optimization algorithm for MSBR core power control. *Nuclear Engineering and Design,* 360(August 2019), 110513. https://doi.org/10.1016/j.nucengdes.2020.110513